

In Silico* Investigations of Some Carbohydrate Derivatives: Pass Prediction, ADMET, QSAR, and Molecular Docking Studies against *Pseudomonas aeruginosa

Ishmam I. Arabi¹ and Sarkar M.A. Kawsar^{2*}

¹Department of Textile Engineering, Green University of Bangladesh,
220/D, Begum Rokeya Sarani, Dhaka 1207 Bangladesh

²Lab of Carbohydrate and Nucleoside Chemistry (LCNC), Department of Chemistry,
Faculty of Science, University of Chittagong, Chittagong 4331 Bangladesh

Carbohydrates are plentiful naturally occurring macromolecules that are crucial to a range of biological activities. Therefore, the focus of our research group has been on computational studies of previously synthesized methyl α -D-glucopyranoside (α -MGP) derivatives. To determine the chemical descriptors of the synthesized compounds, quantum chemical research was conducted using Gaussian09 and the DFT (density functional theory) calculations. Frontier molecular orbital features, electrostatics potential, and thermodynamic properties of these optimized compounds are investigated. PASS (prediction of activity spectra for substances) showed the excellent thermodynamic and antimicrobial properties of the designed α -MGP derivatives. The binding energy and binding strategies of certain bacterial proteins from *Pseudomonas aeruginosa* (3PBN, and 3PBS) were investigated using molecular docking simulations, and adequate binding affinity was reported. QSAR (quantitative structure-activity correlations) analysis found a better drug-likeness profile for all α -MGP derivatives, and pharmacokinetic prediction demonstrated an enhanced drug-likeness profile of α -MGP derivatives. Furthermore, by side chain alteration in the α -D-glucopyranoside sequence, these compounds can be thought of as strong antibacterial agents.

Keywords: ADMET, DFT, glucopyranoside, molecular docking, pharmacokinetic, QSAR

INTRODUCTION

Carbohydrates (sugars or saccharides) are extremely prevalent in nature and have a variety of biological purposes. In nature, sugar can be found both alone and as a component of glycoconjugates, which are essentially glycolipids and glycoproteins (Lysek and Vogel 2006; Staron *et al.* 2018). Carbohydrates have long been a popular research topic among scientists due to their role in biological systems such as viral and bacterial infections, cell growth and proliferation, anticoagulant, antigen, cell-cell communication, immunological response, and

hormones due to their heir highly specific interaction with the physiological receptors (Bertozzi and Kiessling 2001). In addition to providing metabolic energy, they are crucial for sustaining cell-cell interaction and other fundamental activities (Carmona *et al.* 2003). A review of the literature revealed that a significant proportion of physiologically active compounds have aromatic, heteroaromatic, and acyl substituents (Arifuzzaman *et al.* 2018). It is generally known that benzene, substituted benzene, as well as substituents comprising nitrogen, sulfur, and halogens increase the biological activity of the parent molecule (Bulbul *et al.* 2021a; Kawsar *et al.* 2015). It is also recognized that when two active nuclei are combined,

*Corresponding author: akawsarabe@yahoo.com

the new molecule may have more potential for biological activity (Arifuzzaman *et al.* 2018). Furthermore, the combination of two or more heteroaromatic nuclei and acyl groups frequently greatly boosts biological activity as compared to the parent nucleus, according to analyses of microbiological activity and selective acylation of carbohydrates (Kawsar *et al.* 2009; Misbah *et al.* 2020).

Computational drug discovery is a successful technique for speeding up and lowering the cost of drug discovery and development. The usefulness of computational drug development has been expanded due to the enormous rise in the availability of biological macromolecule and small molecule information. Chemical issues can be solved using computer simulations in the field of computational chemistry. Through the use of effective computer tools and theoretical chemistry techniques, it calculates the physicochemical characteristics of the substances (Alam *et al.* 2021; Bulbul *et al.* 2021b; Chen and Fukuda 2006; Maowa *et al.* 2021a). Chemical descriptors such as HOMO-LUMO energy gap, ionization potential, electronegativity (χ), electron affinity (A), chemical potential (μ), electrophilicity (ω), hardness (η), softness (σ), DOS plot, and molecular electrostatic potential (MESP) have been calculated to know their chemical characteristics (Islam *et al.* 2022; Kawsar *et al.* 2020a; Maowa *et al.* 2021b; Rana *et al.* 2021). Based on the molecular structures of drug-like compounds, the computer software ADMET determines the pharmacokinetic parameters and/or characteristics of those substances (Amin *et al.* 2022; Bhargava *et al.* 2011; Gao *et al.* 2010; Hosen *et al.* 2022; Kawsar *et al.* 2021; Shamsuddin *et al.* 2021; Singh *et al.* 2023). The SwissADME web tool is free software that is used to predict the physicochemical properties, absorption, distribution, metabolism, elimination, and pharmacokinetic aspects of molecules – all of which are significant considerations in upcoming clinical research. It takes into account six physicochemical properties – which are very vital, like lipophilicity, flexibility, saturation, polarity, solubility, and size (Dearden 2017; Farhana *et al.* 2021; Hosen *et al.* 2021; Schultz *et al.* 2003). This research can serve as a springboard for laboratory synthesis and facilitate an understanding of experimental results. Quantitative structure-activity correlations (QSARs) is a model that can be used to predict the physicochemical and biological properties of molecules, respectively (Kawsar *et al.* 2008; Luis *et al.* 2007). The biological activity of a new or untested chemical can be inferred from the molecular structure or other attributes of related compounds whose activities have already been evaluated, which is the basis for any QSAR. Changes in a chemical's structure can alter the type and potency of its hazardous effect; hence, models such as structure-activity relationships are used to depict, explain, and, most importantly, forecast phenomena of interest (Ahmmed *et al.* 2023). The QSAR approach provides a

rapid possibility to fulfilling data gaps for limited or absent experimental information. This computational method was applied successfully in different areas such as drug development, toxicity, and pharmacy (Alam *et al.* 2022; Kawsar *et al.* 2020b; Lien *et al.* 1982). In this research, we have focused on the computational studies of previously synthesized methyl α -D-glucopyranoside (α -MGP) and its derivatives. The compounds have been optimized and their thermal, electrical stability, and biochemical behavior have been assessed based on quantum mechanical methods. The thermodynamic and electrical properties are predicted using the B3LYP technique using the basis set 3–21G. Hyperchem software was used to calculate QSAR parameters of molecules such as charge density, surface area grid, volume, Log P, polarizability, refractivity, and molecular mass.

EXPERIMENTAL

Methods

The following software systems were used in the present study: [i] Gaussian 09, [ii] Gausssum 3.0, [iii] AutoDock, [iv] 4.2.6 Swiss-Pdb 4.1.0, [v] Discovery Studio 3.5, [vi] PyMOL 2.3, [vii] LigPlot⁺ v.1.4.5, [viii] Hyperchem, and [ix] Webmo.

Optimization

This study was carried out on a series of molecules using the Gaussian 09 program (Frisch *et al.* 2009). The structures were drawn in GaussView 6. The initial step in getting the leading characteristic parameters of the compounds is to optimize the molecular structure to attain a configuration characterized by minimum free energy through DFT (density functional theory) along with the B3LYP method using a basis set 3–21G. After the completion of the optimization, these structures were used for the calculation of their chemical reactivity descriptors, ADMET, QSAR, and molecular docking.

Calculations of Chemical Reactivity Descriptor

To get the values of chemical reactivity and related descriptors, numerous calculation formulae in acceptable forms were used (Becke 1988; Lee *et al.* 1988). The energy gap, $\Delta\epsilon$ was calculated as $\epsilon\text{LUMO}-\epsilon\text{HOMO}$. Similarly, ionization potential is $I = -\epsilon\text{HOMO}$, electron affinity is $A = -\epsilon\text{LUMO}$, and electronegativity is $\chi = (I + A)/2$. Additionally, chemical potential is μ from $-(I + A)/2$, hardness is $\eta = (I - A)/2$, and electrophilicity is $\omega = \mu^2/2\eta$. Finally, softness, σ was calculated as $1/\eta$. We have used GaussSum 3.0 to get the DOS plot. To visualize MEP, the WebMO demo server (<https://www.webmo.net>) was used.

PASS Prediction

Web-based PASS (prediction of activity spectra for substances; <http://www.pharmaexpert.ru/PASSonline/index.php>) was used for the prediction of a plethora of biological activities. This tool was created to predict a wide range of biological processes with 90% accuracy (Kumaresan *et al.* 2015). ChemDraw 16.0 was used to construct the structures, which were then converted into Smiles format and utilized to predict the biological spectrum using the PASS online version (Kawsar *et al.* 2022a). The result was presented as Pa (probability for active compound) and Pi (probability for inactive compound). Here, $Pa > Pi$ is considered on the scale of 0.000–1.000, and in general, $Pa + Pi \neq 1$. The PASS prediction results were interpreted and used in a flexible manner – such as [i] when $Pa > 0.7$, the chance to find the activity experimentally is high; [ii] if $0.5 < Pa < 0.7$, the chance to find the activity experimentally is less, but the compound is probably not so similar to known pharmaceutical agents; and [iii] if $Pa < 0.5$, the chance to find the activity experimentally is less but not the chance to find structurally (Filimonov *et al.* 2014). Hence, the predicted activity of the spectrum is known as the intrinsic property of the compound.

Protein Preparation and Visualization

The crystal 3D format of some *Pseudomonas aeruginosa* protein (PDB ID: 3PBN and 3PBS) was recuperated in the pdb from the protein data bank (<http://www.ecsb.org>). Using PYMOL software (Version: 2.5.3), the water molecules and extra ligands that had previously been linked to the protein were removed to produce the raw protein strain for molecular docking. The proteins were then subjected to energy minimization by using Swiss-Pdb Viewer (version 4.1.0).

In Silico Pharmacokinetics ADMET and Drug-likeness Parameters Prediction

Computer simulation is used in computational chemistry to aid in the resolution of chemical problems. It computes the physicochemical parameters of the generated molecules using theoretical chemistry approaches embedded in efficient computer algorithms (Islam *et al.* 2019). It can predict many properties of molecules and reactions such as molecular energies and structures, transition state structures, bond and reaction energies, molecular orbitals in different solvent phases, vibrational frequencies, thermo-chemical properties, reaction pathways, spectroscopic quantities, and many other molecular properties for systems in the solid, gas, or solution phase (Luis *et al.* 2007). ADMET is a computer tool designed to estimate pharmacokinetic parameters/properties of drug-like substances based on their molecular structures (Sim *et al.* 1992). SwissADME web tool

(<http://www.swissadme.ch>) is freely available software utilized to predict the physicochemical properties, absorption, distribution, metabolism, elimination, and pharmacokinetic properties of molecules, which are key determinants for more clinical trials. It considers six critical physicochemical properties: lipophilicity, flexibility, solubility, and size. This study can be used to generate a starting point for a laboratory synthesis and to aid in the comprehension of experimental findings.

QSAR Analysis

QSAR is a quantum chemistry approach for linking a compound's biological activity to its molecular structure. It has been widely used as a technique in rational drug design. One of the most important fields in chemometrics is QSARs. QSAR models are mathematical equations that relate chemical structure to biological activity (Ononamadu and Ibrahim 2021). The purpose of QSAR is to connect a molecular structure or molecular structure-derived properties to a specific chemical or biological activity. All the structures were converted into PDB format and the QSAR properties were calculated by Hyperchem Professional software (Version: 8.0.1).

Molecular Docking Studies

In the PyRx the proteins (macromolecules) and ligands were opened. The ligands after energy minimization were converted into PDBQT format. Both the protein and ligands were then forwarded for docking with maximum box size in the Vina wizard. The size of the grid box in AutoDockVina was kept at 28.7131, 23.1244, 30.9032 Å for 3PBN; 29.5830, 22.6536, 27.5685 Å along x, y, and z directions, respectively. The resulting file was saved and further analyzed with the BIOVIA Discovery Studio Visualizer.

RESULTS AND DISCUSSION

The modified derivatives of α -MGP used in this study were designated previously synthesized and represented the structure of the compounds in Figure 1.

PASS Prediction

It seems that a large number of research projects does not reach the final stage because severe unfavorable side effect and toxicity are unknown, and this unfavorable effect is found or arise far too late. But today, in this modern age, it is possible to predict more than 3678 pharmacological effects, modes of action, carcinogenicity, teratogenicity, and other biological properties of compounds using an easy online server named PASS Online (Kumaresan *et al.* 2015). PASS results in their designated Pa and Pi form are presented in Table 1. PASS prediction of Compounds 1–9

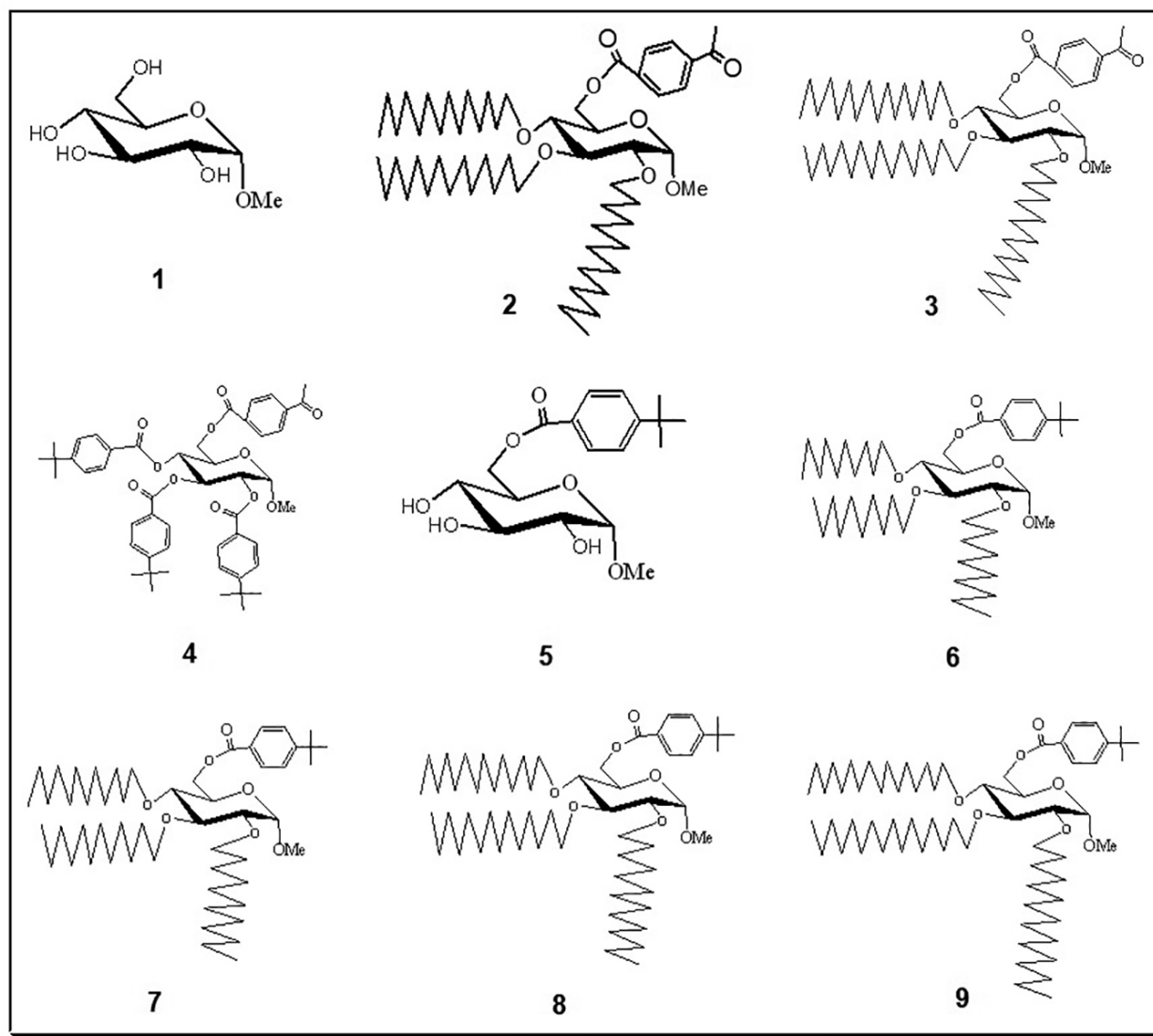


Figure 1. Chemical structure of the methyl α -D-glucopyranoside (α -MGP) (1) and its derivatives (2–9).

was found $0.21 < Pa < 0.50$ in antiviral, $0.39 < Pa < 0.51$ in antibacterial and $0.50 < Pa < 0.73$ in antifungal (Acharya and Rebary 2010; Kabir *et al.* 2008, 2009; Marinescu *et al.* 2015). This indicated that the compounds were more potent against fungi as compared to that bacterial and viral pathogens. We have extended our studies for anti-carcinogenic and antibiotic evaluation.

Thus, PASS prediction indicated $0.69 < Pa < 0.90$ for anti-carcinogenic and $0.22 < Pa < 0.34$ for an antibiotic, which refers that the mannopyranoside derivatives were more potent as anti-carcinogenic agents than that antibiotic properties.

Optimized Structures of the Tested Ligands

The produced ligands' chemical characteristics were further examined using the DFT method for their

quantum calculation and their geometry optimization. The optimized geometrical structure of all synthesized compounds is mentioned in Figure S1.

Chemical Descriptors

Molecular orbitals reveal important details regarding electronic structure. The energy values of the most occupied and least occupied molecular orbitals were computed using the DFT method (Aihara 1999). Molecules with a smaller orbital gap appear to be more polar and have lower efficacy, whereas molecules with the greatest $E(\text{gap})$ indicate the greatest stability (Amin 2013) and are considered softer molecules (Murray and Politzer 2017). The chemical potential (μ), hardness (h), softness (σ), and electrophilicity coefficient (ω) help to determine the biological activity of the lead compound (Amin 2013). Secondly, chemical potential, the positive

Table 1. Data of pass prediction.

Entry	Antiviral		Antibacterial		Antifungal		Antibiotic		Anticancer	
	Pa	Pi	Pa	Pi	Pa	Pi	Pa	Pi	Pa	Pi
1	0.506	0.004	0.541	0.013	0.628	0.019	0.380	0.005	0.574	0.010
2	0.644	0.010	0.494	0.017	0.646	0.017	0.254	0.019	0.575	0.051
3	0.644	0.010	0.494	0.017	0.646	0.017	0.254	0.019	0.575	0.051
4	0.653	0.009	0.478	0.018	0.619	0.017	0.267	0.018	0.723	0.022
5	0.736	0.004	0.481	0.018	0.636	0.015	0.290	0.015	0.653	0.034
6	0.632	0.010	0.441	0.023	0.642	0.014	0.229	0.023	0.594	0.046
7	0.632	0.010	0.441	0.023	0.642	0.014	0.229	0.023	0.594	0.046
8	0.632	0.010	0.441	0.023	0.642	0.014	0.229	0.023	0.594	0.046
9	0.632	0.010	0.441	0.023	0.642	0.014	0.229	0.023	0.594	0.046

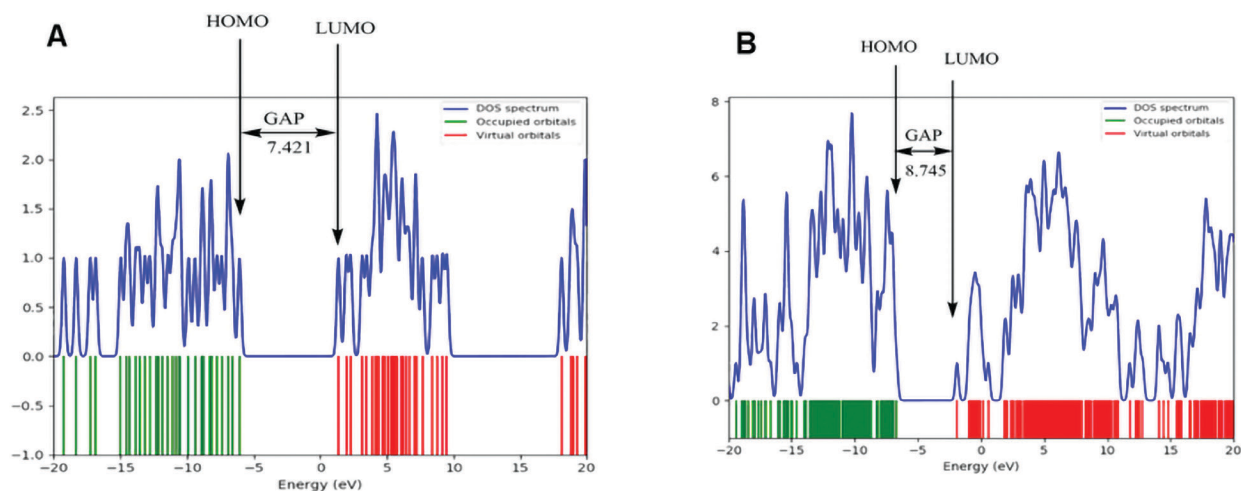


Figure 2. DOS plot representing the HOMO-LUMO gap of Compounds 1 and 4.

Table 2. Data of chemical descriptors.

Entry	ϵ_{LUMO}	ϵ_{HOMO}	$\Delta\epsilon$	A	I	μ	η	χ	ω	σ
1	1.371	-6.050	7.421	-1.371	6.050	-2.339	3.711	2.339	0.737	0.134
2	-2.239	-5.850	3.611	2.239	5.850	-4.044	1.806	4.044	4.527	0.276
3	-2.312	-5.788	3.476	2.312	5.788	-4.054	1.738	4.054	4.728	0.287
4	-1.260	-10.005	8.745	1.260	10.005	-5.632	4.373	5.632	3.626	0.114
5	-1.435	-6.062	4.627	1.435	6.062	-3.748	2.314	3.748	3.035	0.216
6	-1.046	-6.171	5.125	1.046	6.171	-3.608	2.562	3.608	2.540	0.195
7	-1.083	-6.607	5.524	1.083	6.607	-3.845	2.762	3.845	2.676	0.181
8	-0.291	-6.212	5.921	0.291	6.212	-3.252	2.960	3.252	1.786	0.168
9	-1.093	-6.061	4.968	1.093	6.061	-3.577	2.484	3.577	2.575	0.201

*[LUMO] lowest unoccupied molecular orbital; [HOMO] highest occupied molecular orbital; values in eV

chemical potential mainly related to stability and when the softness is lower than hardness, this means the compounds are highly stable. The smaller the energy gap $\Delta\epsilon$ the greater the reactivity of a molecule. Among the compounds, Compound 2 showed a maximum HOMO-LUMO gap (8.745, 7.421 eV). The HOMO-LUMO gaps

of Compounds 4 and 6 are shown in Figure 2 in the form of a DOS plot. The overall frontier molecular orbitals (HOMO, LUMO) value is given in Table 2.

Frontier Molecular Orbitals

Figure S2 illustrates the frontier orbital depiction of

HOMO and LUMO labeling by color. In HOMO, the deep green hue indicates the positive node, whereas the radish color represents the negative node. In the instance of LUMO, the yellow color indicates the negative portion of the orbital, whereas the lightest maroon color represents the positive portion of the orbital. With a specific-colored image in Figure S2, all additional molecules may be found and accessed. According to the findings, HOMO appears to be positioned at the terminal of the benzene ring, which could explain the aromatic ring resonance phenomenon. The presence of an oxygen atom is caused by the presence of LUMO, whereas the presence of a benzene ring and an alkyl group indicates the presence of HOMO.

Molecular Electrostatic Potential (MEP) Map

The molecular electrostatic potential (MEP) is extensively used as a reactivity map that identifies the best region for organic compounds to undertake electrophilic and nucleophilic reactions with charged point-like reagents (Amin 2013). It aids to explore the biological recognition process and hydrogen bonding interaction (Murray and

Politzer 2017). MEP counter maps are a quick and easy approach to estimating how different geometry will interact. The MEP of the title compound is obtained based on the B3LYP with basis set 3-21G optimized result and shown in Figure 3. The primary significance of MEP is that it concurrently displays positive, negative, and neutral electrostatic potential regions, as well as molecule size and shape by color grading, and is extremely valuable in the study of molecular structure with physicochemical properties related (Matta 2014). The different colors of electrostatic potential indicate different values. The potentiality of the attacking zone decreases in the sequence of blue > green > yellow > orange > red. The maximum negative area is indicated by red color, where electrophiles can readily attack, whereas the maximum positive area is indicated by blue color, where nucleophilic assault is possible. Furthermore, the green color indicated that there were no potential zones. Webmo, a free internet program, was used to visualize the MEP images.

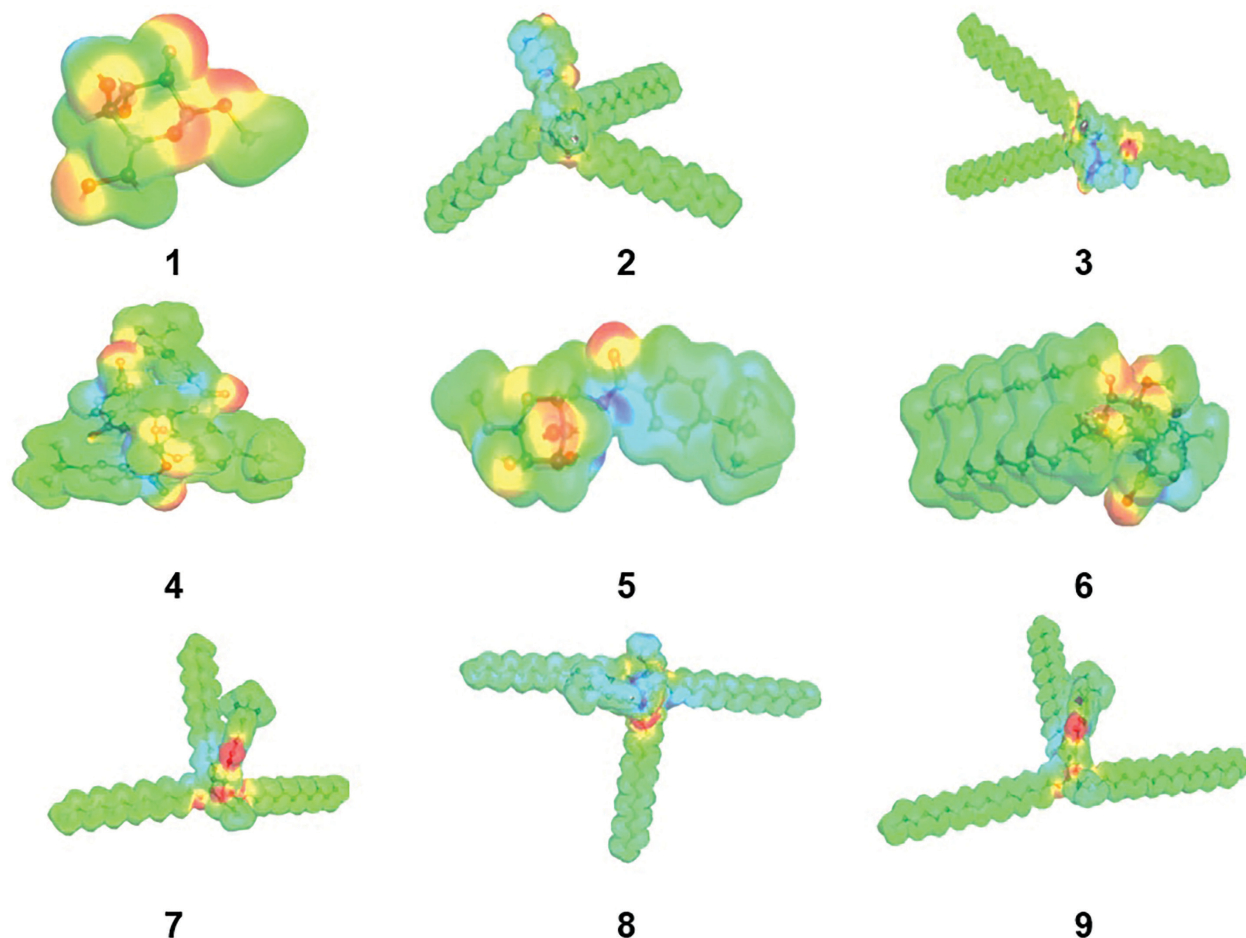


Figure 3. Molecular electrostatic potential (MEP) mappings.

Pharmacokinetic Prediction

For predicting the pharmacokinetic properties of drug/drug-like compounds from their structures, ADMET Predictor – a designed computer program – can be used. A drug/drug-like compound has to satisfy the “Rule of Five” (Lipinski *et al.* 2001), which is a well-known parameter to examine whether it can be taken as a drug or not (Pires *et al.* 2015). Hence, ADMET properties of the synthesized compounds were evaluated using the SwissADME web tool (Tripathi *et al.* 2019), a freely available software utilized to predict the physicochemical properties, absorption, distribution, metabolism, elimination, and pharmacokinetic properties of molecules (Mahanthesh *et al.* 2020). The physicochemical properties of the synthesized ILs can be revealed from ADMET analysis, which includes the rules of five (MW, iLOGP, HBAs, and HBDs) and several other properties like molecular polar surface area (TPSA), number of rotatable bonds (ROTBs), number of aromatic heavy atoms, and number of alerts for undesirable substructures (PAINS and Brenk), among others, as represented in Table 3. All the compounds were by rules, which means MW, RB, HBD, HBA, TPSA, iLOGP, nAH, and MR of all compounds are within the acceptable range. Hence, we can say that all the compounds possess a good pharmacokinetic profile.

QSAR Studies

The QSAR analysis of the compounds is given in Table S1. Hydrophilicity is indicated by a negative Log P value, whereas hydrophobicity is shown by a positive Log P value, both of which are crucial in biochemical interactions and bioactivity. Because hydrophobic medications are maintained for longer, have a wider distribution throughout the body, are less selective in their molecule binding, and are frequently digested, they are

more hazardous. PIC₅₀ value (Table 4) was calculated from the Hyperchem simulation value using the following equation (Bhargava *et al.* 2011) and listed in Table 4.

Table 4. Calculated PIC₅₀ properties of the compounds (1–9).

Entry	PIC ₅₀ value
1	-5.43
2	-30.66
3	-30.25
4	-89.46
5	-25.83
6	-24.53
7	-25.61
8	-25.56
9	-26.76

$$PIC_{50} = 3.028 - 0.542 \text{ Log}P + 0.352 \text{ HE} - 1.272 \text{ Pol} + 0.863 \text{ MR} - 0.038 \text{ MV} - 0.024 \text{ MW} + 19.120q01 + 0.024\text{SAG}$$

Here, [HE] hydration energy, [Pol] polarizability, [MR] molecular refractivity, [Log P] partition coefficient, [MV] molar volume, [MW] molar weight, [SAG] surface area grid, and [q01] atomic net charges.

Molecular Docking Studies and Ligand-Protein Interactions

Molecular docking is an important computational technique in structural biology and computer-aided drug design. The primary goal of molecular docking is to identify potential binding geometries of a putative ligand with a known three-dimensional structure with

Table 3. Calculated ADMET properties of the compounds (1–9).

Entry	MW	HBD	HBA	TPSA (Å ²)	RB	nheavy atoms	MR	PAINS (alert)	Brenk (alert)	GI absorption
1	194.18	4	6	99.38	2	13	40.47	0	0	Low
2	929.46	0	8	89.52	48	66	281.96	0	0	Low
3	1013.62	0	8	89.52	54	72	310.80	0	0	Low
4	820.98	0	11	140.73	18	60	227.03	0	0	Low
5	354.40	3	7	105.45	6	25	89.37	0	0	High
6	775.21	0	7	72.45	36	55	233.35	0	0	Low
7	859.37	0	7	72.45	42	61	262.20	0	0	Low
8	943.53	0	7	72.45	48	67	291.04	0	0	Low
9	1027.69	0	7	72.45	54	73	319.88	0	0	Low

a target protein (Fujii *et al.* 2011; Kawsar *et al.* 2022b). We have selected *Pseudomonas aeruginosa* as the target protein it is an important opportunistic human pathogen that causes severe infections in immunocompromised patients and also in cystic fibrosis patients (Harper and Enright 2011). Molecular docking of the compounds (1–9) was conducted against *Pseudomonas aeruginosa* (PDB ID: 3PBN, 3PBS). The docking scores are shown in Table 5. Initially, molecular docking was conducted with 3PBN, which is a one-chain structure. It was found that Compounds 4 and 5 showed a comparatively binding affinity of -5.7 and -5.5 kcal/mol. Then, 3PBS was used for molecular docking, which is also a one-chain structure. Compound 5 (-5.0 kcal/mol) showed comparatively better binding affinities as compared to the other compounds. The docking score indicated that these compounds possess lower binding affinity as compared to the standard drug ampicillin. These compounds can also act as a quite potent

Table 5. Molecular docking score (binding energy) of Compounds 1–9.

Entry	3PBN	3PBS
1	-4.4	-3.9
2	-4.2	-3.3
3	-4.4	-3.2
4	-5.7	-4.6
5	-5.5	-5.0
6	-4.2	-3.6
7	-4.3	-3.5
8	-4.1	-4.0
9	-4.0	-4.3
Ampicillin	-6.3	-7.6

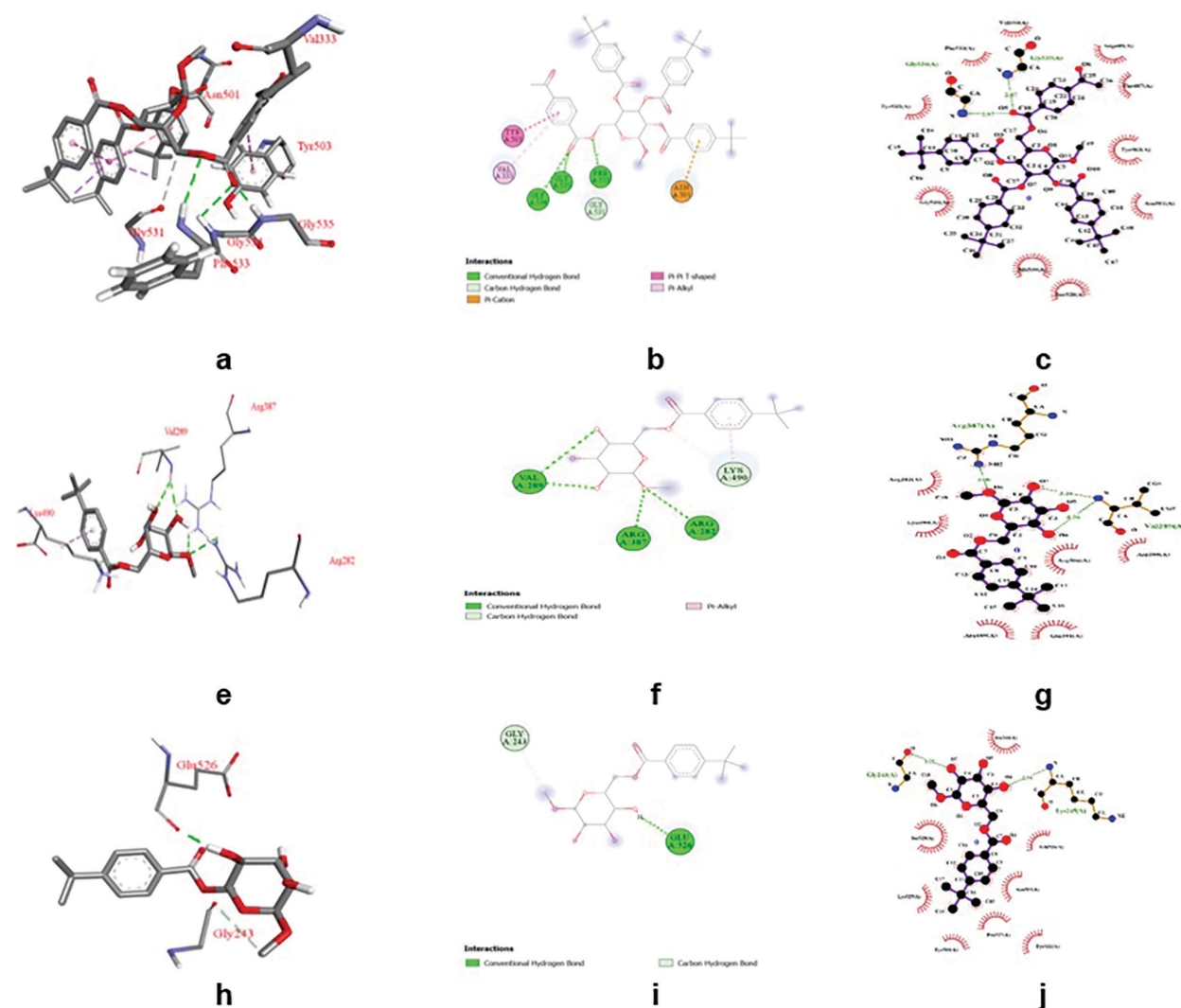


Figure 4. Docking interactions of Compound 4 with 3PBN (a,b,c) and Compound 5 with 3PBN (e, f, and g) and 3PBS (h, i, and j).

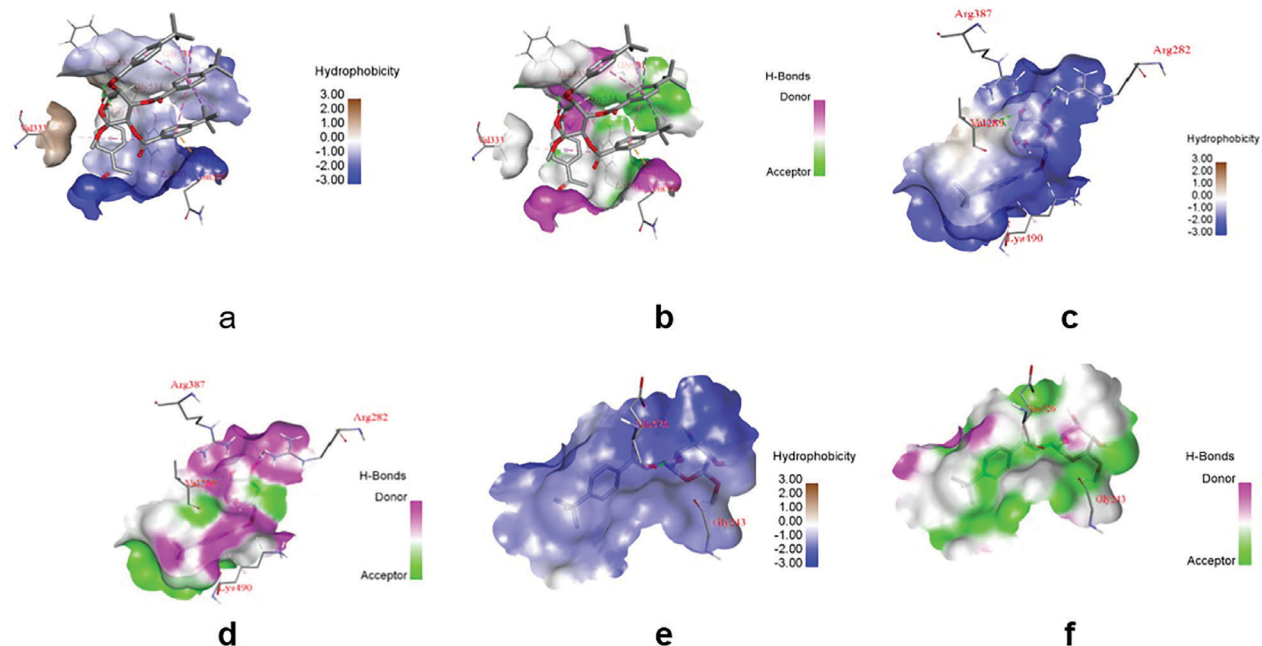


Figure 5. Hydrogen bond and hydrophobic surface of Compound **4** with 3PBN (a and b) and Compound **5** with 3PBN (c and d) and 3PBS (e and f).

drug against *P. aeruginosa* protein by side chain alteration in the α -D-glucopyranoside sequence (Table 5).

Non-bonding interactions of Compounds **4**, and **5** are generated by BIOVIA Discovery Studio, and a two-dimensional image was generated by LigPlot⁺ v.1.4.5. Non-bonding interactions and two-dimensional images are shown in Figure 4.

Figure 5 represents the hydrogen bonds and hydrophobic surface of Compound **4** with 3PBN (a and b) and Compound **5** with 3PBN (c and d) and 3PBS (e and f). These pictures are generated by BIOVIA Discovery Studio. Hydrogen bonds execute a vital function in shaping the specificity of ligand binding with the receptor, drug design in chemical and biological processes, molecular recognition, and biological activity. Figure 5 reveals that all the compounds contain hydrogen bonds and hydrophobic bonds. However, it has been found that the number of hydrogen bond is less than hydrophobic bonds against all proteins, but the hydrogen bonds is stronger than hydrophobic bonds to bond distance (Kawsar *et al.* 2023, 2011). Due to hydrogen-bond forming characteristics, the compounds may act as anti-*P. aeruginosa* drugs.

CONCLUSIONS

In this study, nine glucopyranoside derivatives were studied computationally for their chemical reactivities and molecular docking. Different reactivity parameters

like energy gap ($\Delta\epsilon$), ionization potential (I), electron affinity (A), electronegativity (χ), hardness (η), chemical potential (μ), electrophilicity (ω), and softness (S) indicated that these compounds have moderate reactivities. PASS prediction indicated that these compounds have antiviral, antibacterial, antifungal, antibiotic, and anticarcinogenic characteristics. According to ADMET and QSAR results, these compounds exhibit features that make them likely to be drugs. Molecular docking against *P. aeruginosa* (3PBN and 3PBS) was performed for their antibacterial activity. Among all of the compounds, Compounds **4** and **5** showed comparatively better binding affinities against 3PBN and 3PBS, respectively. However, based on their binding affinities, it is possible that these compounds won't have the same therapeutic effect as ampicillin. A powerful medication against *P. aeruginosa* might be produced by changing the side chain. A larger HOMO-LUMO gap could explain the moderate predicted biological potentiality. As a result, the current study may be useful in the development of glucopyranoside-based antibacterial drugs.

AUTHORS' CONTRIBUTIONS

[Concept] I.I.A., S.M.A.K.; [Design] I.I.A.; [Supervision] S.M.A.K.; [Resources] S.M.A.K.; [Materials] I.I.A., S.M.A.K.; [Data collection and/or processing] I.I.A.; [Analysis and/or interpretation] I.I.A., S.M.A.K.; [Literature search] I.I.A., S.M.A.K.; [Writing] I.I.A., S.M.A.K.; [Critical reviews] S.M.A.K.

ACKNOWLEDGMENTS

The authors are grateful to the Ministry of Science and Technology, Government of the People's Republic of Bangladesh for providing financial support [Ref. (Phy's-591, 2021-2022)] to carry out this research project.

STATEMENT ON CONFLICT OF INTEREST

No potential conflict of interest was declared by the authors.

NOTES ON APPENDICES

The complete appendices section of the study is accessible at <https://philjournsci.dost.gov.ph>

REFERENCES

AHMED F, ISLAM AU, MUKHRISH YE, BAKRI YE, AHMAD S, OZEKI Y, KAWSAR SMA. 2023. Efficient antibacterial/antifungal activities: synthesis, molecular docking, molecular dynamics, pharmacokinetic and binding free energy of galactopyranoside derivatives. *Molecules* 28: 219

ACHARYA S, REBARY B. 2010. Study on the interaction of 3,4-dihydroxyphenylalanine (DL-DOPA) with nonionic and ionic surfactants by fluorescence and UV-visible spectroscopy. *J Surf Sci Technol* 26: 95-103.

AIHARA J. 1999. Reduced HOMO-LUMO gap as an index of kinetic stability for polycyclic aromatic hydrocarbons. *J Phys Chem A* 103: 7487-7495.

AMIN ML. 2013. P-glycoprotein inhibition for drug delivery. *Drug Target Insights* 7: 27.

ALAM A, HOSEN MA, FUJII Y, OZEKI Y, KAWSAR SMA. 2021. Synthesis, Characterization, and Molecular Docking Against a Receptor Protein FimH of *Escherichia coli* (4XO8) of Thymidine Derivatives. *J Mex Chem Soc* 65: 256-276.

ALAMA, RANA KM, HOSEN MA, DEY S, BEZBARUAHB, KAWSAR SMA. 2022. Modified thymidine derivatives as potential inhibitors of SARS-CoV: PASS, *in vitro* antimicrobial, physicochemical, and molecular docking studies. *Phys Chem Res* 10: 391-409.

AMIN MR, YASMIN F, DEY S, MAHMUD S, SALEH MA, EMRAN TB, HASAN I, RAJIA S, OGAWA Y, FUJII Y, YAMADA M, OZEKI Y, KAWSAR SMA. 2022. Methyl β -D-galactopyranoside esters as potential inhibitors for SARS-CoV-2 protease enzyme: synthesis, antimicrobial, PASS, molecular docking, molecular dynamics simulations, and quantum computations. *Glycoconjugate J* 38(5): 1-30.

ARIFUZZAMAN M, ISLAM MM, RAHMAN MM, RAHMAN MA, KAWSAR SMA. 2018. An efficient approach to the synthesis of thymidine derivatives containing various acyl groups: characterization and antibacterial activities. *Acta Pharm Sci* 56: 7-22.

BECKE AD. 1988. Density-functional exchange-energy approximation with correct asymptotic behaviour. *Phys Rev A* 38: 3098-3100.

BERTOZZI CR, KIESSLING LL. 2001. Chemical Glycobiology. *Science* 291: 2357.

BHARGAVA BL, YASAKA Y, KLEIN ML. 2011. Computational studies of room temperature ionic liquid-water mixtures. *Chem Commun* 47: 6228-6241.

BULBUL MZH, CHOWDHURY TS, MISBAH MMH, FERDOUS J, SUJAN D, IMTIAJ H, YUKI F, OZEKI Y, KAWSAR SMA. 2021a. Synthesis of new series of pyrimidine nucleoside derivatives bearing the acyl moieties as potential antimicrobial agents. *Pharmacia* 68: 23-34.

BULBUL MZH, HOSEN MA, FERDOUS J, MISBAH MMH, CHOWDHURY TS, KAWSAR SMA. 2021b. Thermochemical, DFT study, physicochemical, molecular docking, and ADMET predictions of some modified uridine derivatives. *Int J New Chem* 8: 88-110.

CARMONAAT, WHIGTMAN RH, ROBINA I, VOGEL P. 2003. Synthesis and glycosidase inhibitory activity of 7-deoxycasuarine. *Helv Chim Acta* 86: 3066-3073.

CHEN S, FUKUDA M. 2006. Cell type-specific roles of carbohydrates in tumor metastasis. *Meth Enzymol* 416: 371-380.

DEARDEN JC. 2017. The history and development of quantitative structure-activity relationships (QSARs). *Int J Quant Struct Relationships* 2: 36-46.

FARHANA Y, AMIN MR, HOSEN MA, BULBUL MZH, DEY S, KAWSAR SMA. 2021. Monosaccharide derivatives: Synthesis, antimicrobial, PASS, antiviral, and molecular docking studies against SARS-CoV-2 inhibitors. *J Cellul Chem Technol* 55: 477-499.

FILIMONOV DA, LAGUNIN AA, GLORIOZOVA TA, RUDIK AV, DRUZHILOVSKII DS, POGODIN PV,

- POROIKOV VV. 2014. Prediction of the biological activity spectra of organic compounds the PASS online web resource. *Chem Hetero Comp* 50: 444–457.
- FRISCH MJ, TRUCKS GW, SCHLEGEL HB, SCUSE-RIA GE, ROBB A, CHEESEMAN JR, SCALMANI G, BARONE V, MENNUCCI M, PETERSSON GA *et al.* 2009. Gaussian 09. Gaussian Inc., Wallingford, CT.
- FUJII Y, KAWSAR SMA, MATSUMOTO R, YASUMITSU H, NAOTO I, DOGASAKI C, HOSONO M, NITTA K, HAMAKO J, MATSUI T, OZEKI Y. 2011. A-D-galactose-binding lectin purified from coronate moon turban, *Turbo (Lunella) coreensis*, with a unique amino acid sequence and the ability to recognize lacto-series glycosphingolipids. *Comp Biochem Physiol* 158B: 30–37.
- GAO T, ANDINO JM, ALVAREZ-IDABOY JR. 2010. Computational and experimental study of the interactions between ionic liquids and volatile organic compounds. *Phys Chem Chem Phys* 12: 9830–9838.
- HARPER DR, ENRIGHT MC. 2011. Bacteriophages for the treatment of *Pseudomonas aeruginosa* infections. *J Appl Microbiol* 111: 1–7.
- HOSEN MA, MUNIANS, AL-GHORBANIM, BAASHEN M, ALMALKI FA, HADDA TB, ALI F, MAHMUD S, SALEH MA, LAAROUSSI H, KAWSAR SMA. 2022. Synthesis, antimicrobial, molecular docking, and molecular dynamics studies of lauroyl thymidine analogs against SARS-CoV-2: POM study and identification of the pharmacophore sites. *Bioorg Chem* 125: 105850.
- HOSEN MA, ALAM A, ISLAM M, FUJII Y, OZEKI Y, KAWSAR SMA. 2021. Geometrical optimization, PASS prediction, molecular docking, and *in silico* ADMET studies of thymidine derivatives against FimH adhesin of *Escherichia coli*. *Bulg Chem Commun* 53: 327–342.
- ISLAM S, HOSEN MA, AHMAD S, UL QAMAR, MT, DEY S, HASAN I, FUJII Y, OZEKI Y, KAWSAR SMA. 2022. Synthesis, antimicrobial, anticancer activities, PASS prediction, molecular docking, molecular dynamics, and pharmacokinetic studies of designed methyl α -D-glucopyranoside esters. *J Mol Struct* 1260: 132761.
- ISLAM MJ, ZANNAT A, KUMER A, SARKER N, PAUL S. 2019. The prediction and theoretical study for chemical reactivity, thermophysical, and biological activity of morpholinium nitrate, ionic liquid crystals: a DFT study. *Adv J Chem A* 2: 316–326.
- KABIR AKMS, KAWSAR SMA, BHUIYAN MMR, RAHMAN MS, BANU B. 2008. Biological evaluation of some octanoyl derivatives of methyl 4,6-O-cyclohexylidene- α -D-glucopyranoside. *Chittagong Univ J Biol Sci* 3: 53–64.
- KABIR AKMS, KAWSAR SMA, BHUIYAN MMR, RAHMAN MS, CHOWDHURY ME. 2009. Antimicrobial screening studies of some derivatives of methyl α -D-glucopyranoside. *Pak J Sci Ind Res* 52: 138–142.
- KAWSAR SMA, KUMAR A, NASRIN SM, HOSEN MA, CHAKMA U, AKASH S. 2022a. Chemical descriptors, PASS, molecular docking, molecular dynamics, and ADMET predictions of glucopyranoside derivatives as inhibitors to bacteria and fungi growth. *Org Commun* 15: 184–203.
- KAWSAR SMA, HOSEN MA. 2020a. An optimization and pharmacokinetic studies of some thymidine derivatives. *Turk Comput Theor Chem* 4: 59–66.
- KAWSAR SMA, FUJII Y, MATSUMOTO R, ICHIKAWA T, TATENO H, HIRABAYASHI J, YASUMITSU H, DOGASAKI C, HOSONO M, NITTA K, HAMAKO J, MATSUI T, OZEKI Y. 2008. Isolation, purification, characterization, and glycan-binding profile of a d-galactoside specific lectin from the marine sponge, *Halichondria okadai*. *Comp Biochem Physiol B Biochem Mol Biol* 150:349–357.
- KAWSAR SMA, HOSEN MA, CHOWDHURY TS, RANA KM, FUJII Y, OZEKI Y. 2021. Thermochemical, PASS, molecular docking, drug-likeness, *in silico* ADMET prediction of cytidine derivatives against HIV-1 reverse transcriptase. *Rev de Chim* 72: 159–178.
- KAWSAR SMA, HOSEN MA, FUJII Y, OZEKI Y. 2020b. Thermochemical, DFT, Molecular Docking, and Pharmacokinetic Studies of Methyl β -D-galactopyranoside Esters. *J Comput Chem Mol Model* 4: 452–462.
- KAWSAR SMA, MATSUMOTO R, FUJII Y, YASUMITSU H, DOGASAKI C, HOSONO M, NITTA K, HAMAKO J, MATSUI T, KOJIMA N, OZEKI Y. 2009. Purification and biochemical characterization of a D-galactose binding lectin from Japanese sea hare (*Aplysia kurodai*) eggs. *Biochem Moscow* 74: 709–716.
- KAWSAR SMA, HAMIDAAA, SHEIKHAU, HOSSAIN MK, SHAGIRAC, SANALLAHAFM, MANCHURMA, IMTIAJH, OGAWA Y, FUJII Y, KOIDE Y, OZEKI Y. 2015. Chemically modified uridine molecules incorporating acyl residues to enhance antibacterial and cytotoxic activities. *Int J Org Chem* 5: 232–245.
- KAWSAR SMA, HOSEN MA, AHMAD S, BAKRI YE, LAAROUSSI H, HADDA TB, ALMALKI FA, OZEKI Y, GOUMRI-SAID S. 2022b. Potential SARS-CoV-2 RdRp inhibitors of cytidine derivatives: molecular docking, molecular dynamic simulations, ADMET, and

- POM analyses for the identification of pharmacophore sites. *PLoS ONE* 17: e0273256.
- KAWSAR SMA, ALMALKI FA, HADDA TB, LAAR-OUSSI H, KHAN MAR, HOSEN MA, MAHMUD S, AOUNTI A, MAIDEEN NMP, HEIDARIZADEH F, SOLIMAN SSM. 2023. Potential antifungal activity of novel carbohydrate derivatives validated by POM, molecular docking, and molecular dynamic simulations analyses. *Mol Simul* 49: 60–75.
- KAWSAR SMA, MATSUMOTO R, FUJII Y, MATSUOKA H, MASUDA N, IWAHARA C, YASUMITSU H, KANALY RA, SUGAWARA S, HOSONO M, NITTA K, ISHIZAKI N, DOGASAKI C, HAMAKO J, MATSUI T, OZEKI Y. 2011. Cytotoxicity and glycan-binding profile of α -D-galactose-binding lectin from the eggs of a Japanese sea hare (*Aplysia kurodai*). *Protein J* 30: 509–5197.
- KUMARESAN S, SENTHILKUMAR V, STEPHEN A, BALAKUMAR BS. 2015. GC-MS analysis and PASS-assisted prediction of biological activity of extract of *Phomopsis* sp. Isolated from *Andrographis paniculata*. *World J Pharm Res* 4: 1035–1053
- LEE C, YANG W, PARR RG. 1988. Development of the Colle-Salvetti correlation-energy formula into a functional of the electron density. *Phys Rev B* 37: 785–789.
- LIEN EJ, GUO ZR, LI RL, SU CT. 1982. Use of dipole moment as a parameter in drug-receptor interaction and quantitative structure-activity relationship studies. *J Pharm Sci* 71: 641–655.
- LIPINSKI CA, LOMBARDO F, DOMINY BW, FEENEY PJ. 2001. Experimental and computational approaches to estimate solubility and permeability in drug discovery and development settings. *Adv Drug Deliv Rev* 46: 3–26
- LUIS P, ORTIZ I, ALDACO R, IRABIEN A. 2007. A novel group contribution method in the development of a QSAR for predicting the toxicity (*Vibrio fischeri* EC50) of ionic liquids. *Ecotoxicol Environ Saf* 67: 423–429.
- LYSEK R, VOGEL P. 2006. Synthesis of amino- and diaminoconduritols and their applications. *ChemInform* 62: 2733–2768.
- MAHANTHESH MT, RANJITH D, RAGHAVENDRA Y, JYOTHI R, NARAPPA G, RAVI MV. 2020. Swiss ADME prediction of phytochemicals present in *Butea monosperma* (Lam.) Taub. *J Pharmacogn Phytochem* 9: 1799–1809
- MARINESCU M, EMANDI A, MARTON G, CINT-EZA LO, CONSTANTINESCU C. 2015. Structural studies and optical nonlinear response of some pyrazole-5-ones. *Nanosci Nanotechnol Lett* 7: 846–854
- MATTA CF. 2014. Modeling biophysical and biological properties from the characteristics of the molecular electron density, electron localization, and delocalization matrices, and the electrostatic potential. *J Comput Chem* 35: 1165–1198
- MAOWA J, HOSEN MA, ALAMA, RANA KM, FUJII Y, OZEKI, Y, KAWSAR SMA. 2021a. Pharmacokinetics and molecular docking studies of uridine derivatives as SARS-CoV-2 M^{Pro} inhibitors. *Phys Chem Res* 9: 385–412.
- MAOWA J, ALAM A, RANA KM, DEY S, HOSEN A, FUJII Y, HASAN I, OZEKI Y, KAWSAR SMA. 2021b. Synthesis, characterization, synergistic antimicrobial properties, and molecular docking of sugar modified uridine derivatives. *Ovidius Univ Ann Chem* 32: 6–21.
- MISBAH MMH, FERDOUS J, BULBUL MZH, CHOWDHURY TS, DEY S, HASAN I, KAWSAR SMA. 2020. Evaluation of MIC, MBC, MFC, and anticancer activities of acylated methyl β -D-galactopyranoside esters. *Int J Biosci* 16: 299–309.
- MURRAY JS, POLITZER P. 2017. Molecular electrostatic potentials and noncovalent interactions. *WIREs Comput Mol Sci* 7: e1326.
- ONONAMADUCJ, IBRAHIMA. 2021. Molecular docking and prediction of ADME/drug-likeness properties of potentially active antidiabetic compounds isolated from aqueous-methanol extracts of *Gymnema sylvestre* and *Combretum micranthum*. *BioTechnologia (Pozn)* 102: 85–99.
- PIRES DEV, BLUNDELL TL, ASCHER DB. 2015. pkCSM: Predicting small-molecule pharmacokinetic and toxicity properties using graph-based signatures. *J Med Chem* 58: 4066–4072.
- RANA KM, MAOWA J, ALAM A, DEY S, HOSEN A, HASAN A, HASAN I, FUJII Y, OZEKI Y, KAWSAR SMA. 2021. *In silico* DFT study, molecular docking, and ADMET predictions of cytidine analogs with antimicrobial and anticancer properties. *In Silico Pharmacol* 9: 42.
- SHAMSUDDIN T, HOSEN MA, ALAM MS, EMRAN TB, KAWSAR SMA. 2021. Uridine derivatives: antifungal, PASS outcomes, ADME/T, drug-likeness, molecular docking, and binding energy calculations. *Med Sci Int Med J* 10: 1373–1386.
- SCHULTZ TW, CRONIN MTD, NETZEVA TI. 2003. The present status of QSAR in toxicology. *J Mol Struct* 622: 23–38.
- SIM F, ST-AMANT A, PAPAI I, SALAHUB DR. 1992. Gaussian density functional calculations on hydrogen-bonded systems. *J Am Chem Soc* 114: 4391–4400.

- SINGH R, KUMAR P, SINDHU J, DEVIM, KUMARA, LAL S, SINGH D. 2023. Parsing structural fragments of thiazolidine-4-one based α -amylase inhibitors: a combined approach employing *in vitro* colorimetric screening, GA-MLR based QSAR modelling supported by molecular docking, molecular dynamics simulation, and ADMET studies. *Compt Biol Med* 157: 106776.
- STARON J, DABROWSKI JM, CICHON E, GUZIK M. 2018. Lactose esters: synthesis and biotechnological applications. *Crit Rev Biotechnol* 38: 245–258.
- TRIPATHI P, GHOSH S, TALAPATRA SN. 2019. Bio-availability prediction of phytochemicals present in *Calotropis procera* (Aiton) R. Br. by using Swiss-ADME tool. *World Sci News* 131: 147–163.

APPENDICES

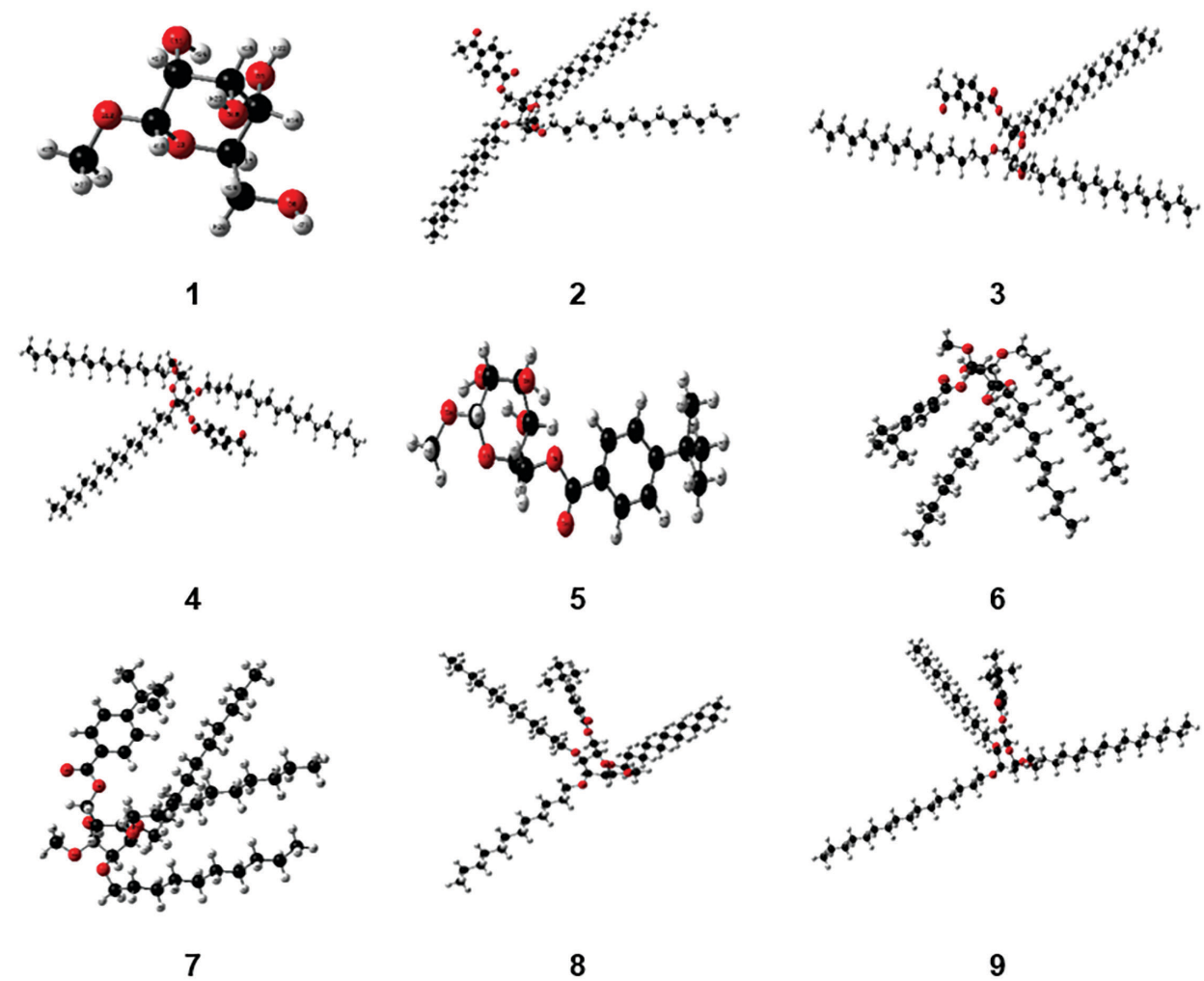


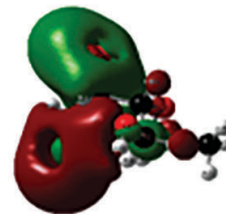
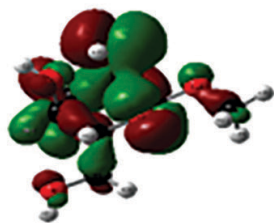
Figure S1. Optimized structures of glucopyranoside derivatives (1–9).

Entry

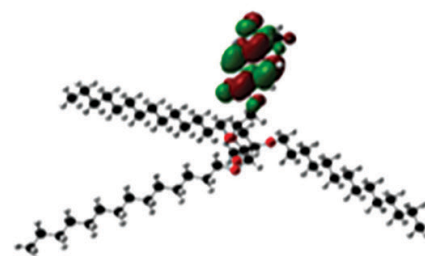
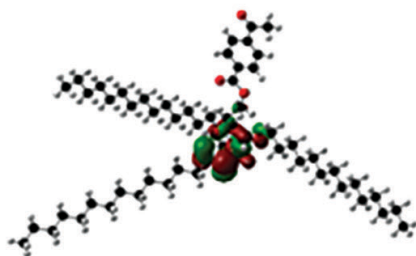
HOMO

LUMO

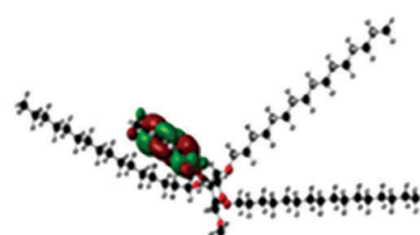
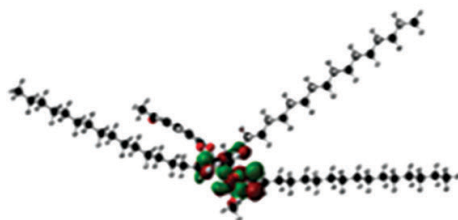
1



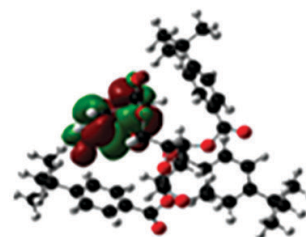
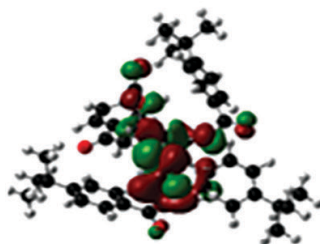
2



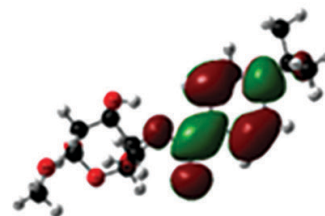
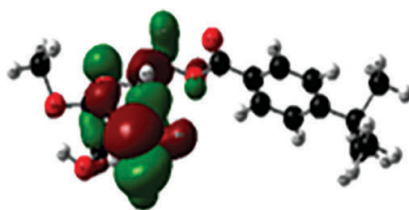
3



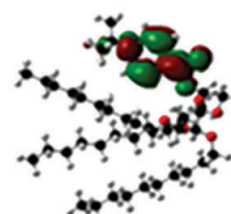
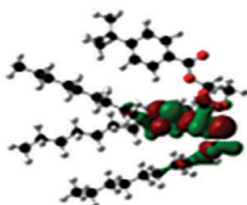
4



5



6



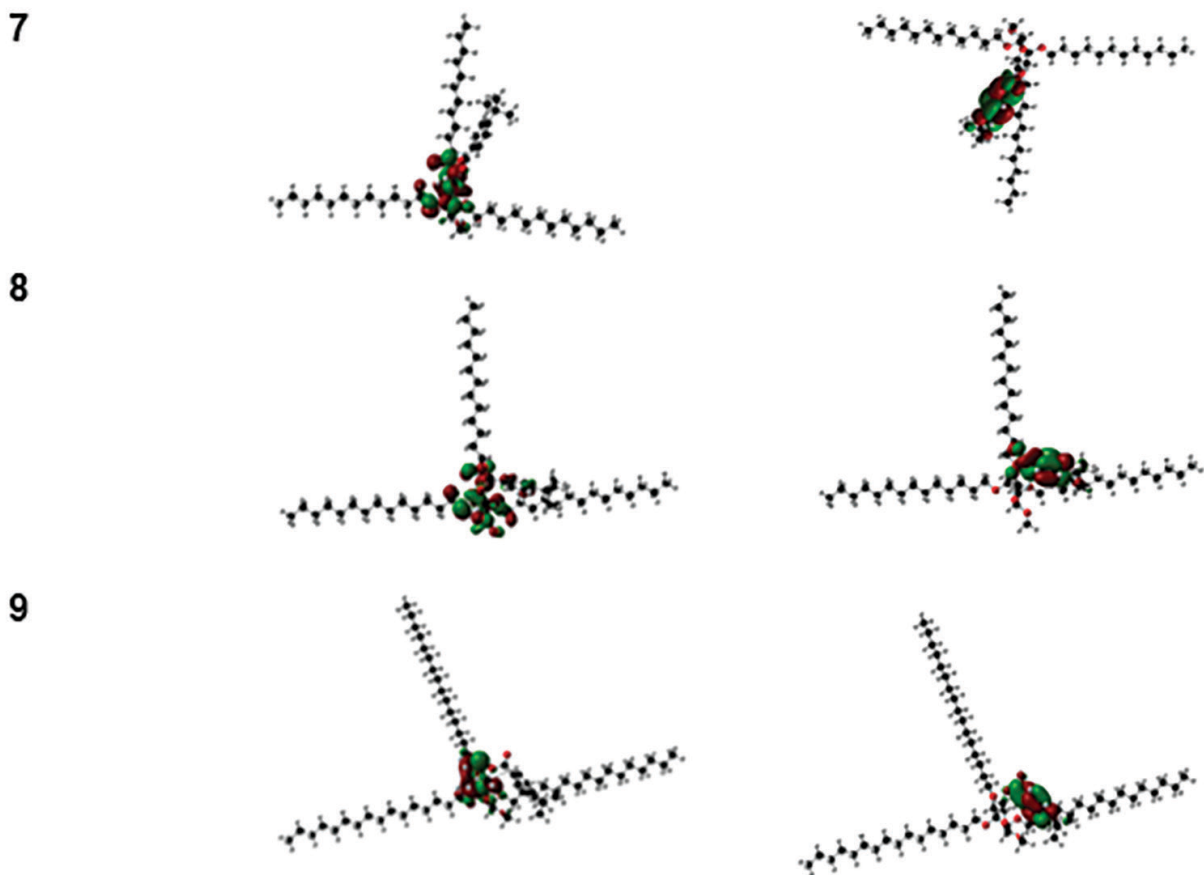


Figure S2. HOMO-LUMO pictures of the compounds.

Table S1. QSAR studies of the compounds (1–9).

Entry	Mass (amu)	Partial charge (e)	Surface area (grid) (Å ²)	Surface area (approx) (Å ²)	Volume (Å ³)	Hydration Energy (Kcal/mol)	Logp	Refractivity (Å ³)	Polarizability (Å ³)
1	194.18	0	358.46	296.39	556.12	-16.96	-1.48	40.67	16.67
2	929.46	0	1795.11	2008.87	3191.90	9.68	20.15	246.83	109.07
3	1013.62	0	1920.42	2134.07	3456.31	12.53	22.53	274.44	120.08
4	820.98	0	975.91	992.61	2057.08	-5.21	19.06	124.03	88.77
5	354.40	0	583.93	524.19	997.08	-13.12	3.60	64.38	35.59
6	775.21	0	1122.81	1308.63	2359.09	5.72	15.19	203.07	90.64
7	859.37	0	1628.75	1821.93	2920.14	10.25	17.57	230.67	101.65
8	943.53	0	1797.76	2005.84	3224.55	13.23	19.95	258.28	112.66
9	1027.69	0	2017.42	2265.82	3583.14	14.86	22.33	285.89	123.67